# McMaster University

## Advanced Optimization Laboratory


**Title:**

Controlling the dose distribution with gEUD-type constraints within the convex IMRT optimization framework

**Authors:**

Y. Zinchenko, T. Craig, H. Keller,
T. Terlaky and M. Sharpe

**AdvOl-Report No. 2007/15**

September 2007, Hamilton, Ontario, Canada

# Controlling the dose distribution with gEUD-type constraints within the convex IMRT optimization framework

Y. Zinchenko[1,2], T. Craig[2], H. Keller[2], T. Terlaky[1] and M. Sharpe[2]

September 26, 2007

**Abstract**

Radiation therapy is an important modality in treating various cancers. Various treatment planning and delivery technologies have emerged to support Intensity Modulated Radiation Therapy (IMRT), creating significant opportunities to advance this type of treatment. We investigate the possibility of including the dose prescription, specified by the Dose Volume Histogram (DVH), within the convex optimization framework for inverse IMRT treatment planning. Specifically, we study the quality of approximating a given DVH with a superset of generalized Equivalent Uniform Dose (gEUD)-based constraints, the so-called Generalized Moment Constraints (GMCs).

The newly proposed approach is promising as demonstrated by the computational study where the rectum DVH is considered. Unlike the precise dose-volume constraint formulation that necessitates the use of expensive computing resources, our convex optimization approach is feasible for implementation on a single-processor treatment planning station.

**Keywords:** IMRT, DVH, gEUD, GMC, inverse planning, convex optimization, generalized moments, Tchebychev inequalities.

[1]AdvOL, Department of Computing and Software, McMaster University
[2]Department of Radiation Oncology, University of Toronto

# 1 Introduction and motivation

Radiation therapy is an important modality in treating various cancers. IMRT, an advanced form of radiation delivery developed over the past two decades, is possible with state-of-the-art tools for optimizing this type of treatment. Treatment planning for IMRT typically involves solving a highly complex inverse problem, often with the use of optimization methods.

Dose prescriptions are frequently expressed in terms of partial-organ doses or a fractional dose-volume histogram, however, a precise implementation of such prescriptions is often associated with great computational difficulties and most often a compromise sub-optimal solution is settled for in practice. We investigate the possibility of including this type of dose prescription within the convex optimization framework for inverse IMRT treatment planning. More precisely, we study the quality of approximating a given DVH with multiple gEUD-type constraints, the Generalized Moment Constraints (GMC). The techniques outlined in this paper are well suited to be embedded into the robust IMRT treatment planning framework [6, 5, 12] – the approach that theoretically allows to minimize the negative impact of inherent uncertainties related to setup error and organ movement.

For a given volume of interest, e.g., an organ at risk or a clinical target volume, a *DVH or Dose-Volume Histogram* specifies the complete dose distribution to the volume with the exception of its spatial information. Namely, for any given dose $T$, the DVH curve in its cumulative form specifies percentage of the total volume $\mathrm{DVH}(T)$ that receives dose greater (or equal) than $T$. Knowing the DVH curve allows us to deduce various aggregate properties of the dose distribution, e.g., an average dose to a unit volume may be computed as a ratio of an integral of $\mathrm{DVH}(T)$ over all possible values of $T$ to the total volume, etc.

*gEUD or Generalized Equivalent Uniform Dose* values in the context of radiation therapy treatment planning were introduced in [11], and have already been studied as an alternative to the DVH-based dose prescription [3, 13]. gEUD-values have the desirable property of being either convex or concave functions of the dose, making them attractive for specifying the treatment plan optimization goals. However, until recently, the modeling capabilities of the gEUD-type constraints were poorly understood. Once the volume of interest is discretized into a collection of voxels $V$, the (discrete approximation to) gEUD value corresponding to the parameter $a$ is computed as $\mathrm{gEUD}_a = \frac{1}{|V|}\sum_{v\in V} {d_v}^a$, with $d_v$ representing a dose to a voxel $v \in V$ and $|V|$ being the total number of voxels.

Surprisingly, the fundamental relationship between the DVH and the gEUD's is given to us by probability theory. The relationship is more general than what we require, so adapted to our needs it may be phrased as follows:

**Fact 1.1.** *Given a DVH, the infinite sequence of values* $\{\mathrm{gEUD}_a\}_{a=1,2,3,\ldots}$*, is determined uniquely. Conversely, the sequence* $\{\mathrm{gEUD}_1, \mathrm{gEUD}_2, \mathrm{gEUD}_3, \ldots\}$*, uniquely determines the DVH.*

For more details and a rigorous derivation please see Section 3 and the Appendix.

The motivation to find an alternative to purely DVH-based dose distribution prescription stems, in part, from the fact that previous attempts to embed such requirements in the treatment planning process were typically associated with immense computational difficulties, and quite frequently, the necessity to resort to an iterative interactive human-to-planning-station process. To give an illustration, consider the following scenario where we introduce a *single-point DVH* constraint.

It is quite common that the planner is asked to find a treatment plan where the DVH for a given organ at risk lies below a certain collection of points -the *critical DVH points*- of the form $(T, P)$ where $T$ is the critical dose value and $P$ is the maximal volume-percentage of the organ that may receive the dose exceeding $T$. Such a requirement may be embedded into the inverse treatment planning model with use of binary variables: let the organ be discretized into collection of voxels $V$, $d_v$ be a dose to a single voxel for $v \in V$, $T$ be one such critical dose value with the corresponding maximal allowed organ volume-percentage $P$, and $M$ be the absolute maximal dose allowed to any voxel in the organ. Then the requirement that the resulting DVH lies below the point $(P, T)$ may be accommodated by adding $|V|$ binary (indicator) variables $i_v$ to the model as follows:

$$\begin{array}{l} d_v \leq T + i_v \cdot (M - T),\ v \in V, \\ \frac{1}{|V|} \sum_{v \in V} i_v \leq P, \\ i_v \text{ is 0 or 1 for all } v \in V. \end{array} \tag{1}$$

Similar procedure would have to be repeated for each critical DVH point, if there is more than one such point. Unfortunately, a set of constraints like the above becomes extremely difficult to handle computationally, with the inherent difficulty mostly due to the discrete nature of the newly introduced binary indicator variables (and hence non-convexity of the problem's feasible region). The worst-case computational difficulty of a problem like this grows exponentially with the number of such discrete variables; roughly speaking, in the worst-case one would need to enumerate all the possible combinations for $i_v$'s to find the solution, thus facing an order of $2^{|V|}$ mathematical operations required. Although our algorithmic capacities to handle particularly structured problems of this type and the sheer computational power have advanced greatly within the past few decades, the real-world IMRT application of this approach falls only within the realm of super-computing [9, 10]. In practice, the precise DVH requirements and the constraints like the above are almost never used, and a compromise sub-optimal solution is searched for instead.

Taking into account the above mentioned computational challenge, another point of concern is the physical applicability of just a limited number of single-point DVH constraints as above: suppose we have specified only two critical points on the DVH for the organ, say, at most 50% of the bladder receives dose above 60Gy, while no voxel in the bladder receives a dose above 81Gy. But what may happen in between these two points? In other words, is it ok for 99% of the bladder to receive a dose of 59Gy, or for 49% to receive 80Gy? Obviously, the later would be hardly a desirable outcome of the treatment planning process.

Thus, it is conceivable that one might need to specify a nearly complete dose distribution within the acceptable margins, and indeed, many single-point DVH constraints may be called upon.

From the computational point of view the advantage of using the gEUD-type constraints, as opposed to the above mentioned single-point DVH constraints, is that, in contrast, the gEUD's may allow us to preserve a favorable computational structure, namely, the convexity of the underlying mathematical problem. In turn, this allows for much more efficient (and even polynomial-time in the problem dimensions) algorithms to be used [2, 14]. Fact 1.1 establishes a one-to-one correspondence between an infinite sequence of gEUD values and the prescribed DVH curve. The above has the implication that, if during the treatment planning process we are able to restrict our search space of all possible treatment plans to the ones that correspond to only the prescribed (infinitely many) gEUD values for all $a = 1, 2, 3, \ldots$, then as the result of running an optimization algorithm on such a model we would expect a treatment plan that produces the desired DVH, or, alternatively, a certificate that no such plan exists.

Consequently, the question we want to address is the following: can we start with a desired DVH for various volumes of interest and build those into our inverse treatment planning model, treating $d_v, v \in V$, as (a subset of all) the decision variables, i.e., the variables we can control, and preserving the convexity relying on the statement above?

From now on we consider a single volume of interest discretized into a collection of (iso-volumetric) voxels $V$, with a maximum dose to a voxel bounded by 1. The last assumption is made without loss of generality since any dose distribution may be scaled so that the maximum allowed dose is equal to 1 unit.

For a given $a$ we have

$$\frac{1}{|V|}\sum_{v\in V} d_v^a = \mathrm{gEUD}_a, \tag{2}$$

where

$$\frac{1}{|V|}\sum_{v\in V} d_v^a \text{ is } \begin{cases} \text{convex in } d_v, & \text{if } a \in (-\infty, 0]\bigcup[1,\infty), \\ \text{concave in } d_v, & \text{if } a \in [0,1] \end{cases}$$

(recall that $d_v \geq 0$).

Firstly, to utilize the full power of Fact 1.1 we would have to incorporate infinitely many equality-type constraints (2) into our model, which could be quite challenging. Fortunately, if we are willing to accept some limited deviation from the prescribed "ideal" DVH, we do not need to specify all of the gEUD values: typically just a few will suffice to get a good approximation.

Secondly, in order to preserve the convexity of our model's feasible region, we need to use the inequality-type constraints like

$$\begin{cases} \frac{1}{|V|}\sum_{v\in V} d_v^a \leq \overline{\mathrm{gEUD}}_a, & \text{if } a \in (-\infty, 0]\bigcup[1,\infty), \\ \frac{1}{|V|}\sum_{v\in V} d_v^a \geq \underline{\mathrm{gEUD}}_a, & \text{if } a \in [0,1] \end{cases} \tag{3}$$

with $\overline{\mathrm{gEUD}}_a, \underline{\mathrm{gEUD}}_a$ being some predetermined values, e.g., $d_1^2 \leq 1$ for $a = 2$ and $V = \{1\}$. Unlike the statement of Fact 1.1, now we would have to specify

a range rather than a single gEUD value. Noting that the inequalities in the above may be interpreted as equalities, $\frac{1}{|V|}\sum_{v\in V} d_v^a = \mathrm{gEUD}_a^*$ where $\mathrm{gEUD}_a^* \in [\underline{\mathrm{gEUD}}_a, 1]$ or $\mathrm{gEUD}_a^* \in [0, \overline{\mathrm{gEUD}}_a]$, we expect to observe a whole range of resulting DVH curves that satisfy these constraints.

In what follows we examine the quality of approximating the desired dose distribution specified by DVH with multiple gEUD-type constraints, the Generalized Moment Constraints. If our approach is to be treated as a black box, the input would be the targeted DVH for the volume of interest, and the output would be the set of convex constraints on the dose variables $d_v$, $v \in V$ which, if satisfied, guarantees the approximation of the desired dose distribution within the corresponding error margin. We refer to any dose distribution that satisfies a given set of GMCs on $d_v \geq 0$, $v \in V$ as *feasible*.

**Remark 1.1.** *Fact 1.1 provides means to generate cuts to strengthen a convex relaxation of mixed integer constraints* (1)*. In particular, in Section 4 we describe a second-order cone formulation of moment constraints that bound gEUD values, which can further be well approximated with linear inequalities at modest (polynomial) cost.*

# 2 Two geometric questions about DVH

## 2.1 What is the intuitive interpretation of gEUD-type constraints for DVH?

Consider the following example. Suppose the volume of interest consists of only two voxels, that is, $V = \{1, 2\}$. We would like to investigate all the possible DVH curves that satisfy a single DVH-type equality constraint (2) corresponding to $a = 1$ with the corresponding gEUD value of, say, $\frac{1}{2}$, that is, the DVH curves that come from dose distributions satisfying $\frac{1}{2}(d_1 + d_2) = \frac{1}{2}$. Note that the requirement $d_1, d_2 \geq 0$ is implicit.

Clearly, since only two voxels are considered, each comprising 50% of the total volume, the DVH is a step function with three flat segments corresponding to 100%, 50% and 0% of the volume. The range of all possible values for $d_1, d_2$ satisfying $d_1 + d_2 = 1$ will give us the locations of the first drop of the DVH step function from 100% to 50% and the the second drop from 50% to 0%.

Since the resulting DVH is invariant under re-indexing of $d_1$ and $d_2$, e.g., two distinct distributions $\{d_1 = 1, d_2 = 0\}$ and $\{d_1 = 0, d_2 = 1\}$ result in the same DVH, for the purpose of reconstructing all possible DVH curves that come from feasible dose distributions we may assume $d_2 \geq d_1$. Observe that $\mathrm{DVH}(d_1-) = 1$, $\mathrm{DVH}(d_1+) = 1/2$ together with $\mathrm{DVH}(d_2-) = 1/2$, $\mathrm{DVH}(d_2+) = 0$, see Figure 1; here we adopt the standard calculus notation for $d-$ and $d+$ to mean ever so slightly to the left and to the right from the point $d$ respectively. Also note that once $d_1$ is fixed, $d_2$ is obtained from the gEUD-type equality constraint as $d_2 = 1 - d_1$. Now, ranging $d_1$ from 0 to $\frac{1}{2}$ we may reconstruct all possible DVH curves satisfying $d_1 + d_2 = 1$; note that $d_1$ may not exceed $\frac{1}{2}$ since we assume $d_2 \geq d_1$.

Observe that all the DVH's as described, in addition to being a step functions with two drops from 100% to 50% and from 50% to 0%, must satisfy one and only one requirement: the area under the DVH must be equal to $\frac{1}{2}$. Taking this argument further, if we increase the number of voxels, then obviously the number of possible drops in the DVH is also bound to increase in the limit producing a smooth curve, while the area under the DVH curve has to stay unchanged, and thus, any DVH such that $\int_0^1 \mathrm{DVH}(x)dx = \frac{1}{2}$ would correspond to a feasible distribution.

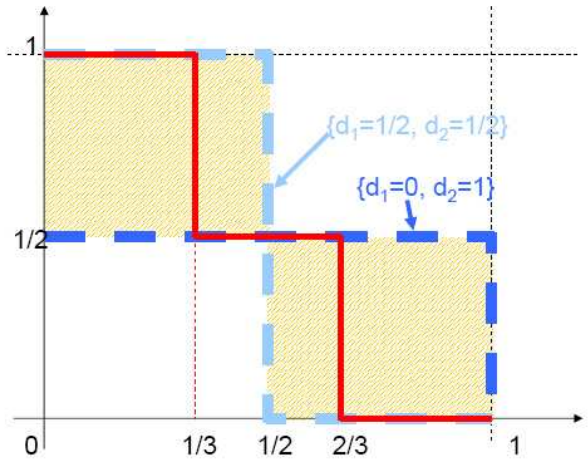


Figure 1: A family of DVH curves satisfying a gEUD-type equality constraint.

The bottom line in the above example is that any gEUD-type constraint imposes some restrictions on the resulting DVH curve. It is that by carefully superimposing several such gEUD-type constraints one hopes to achieve the desired quality of approximation to the ideal DVH.

Based on the shape of the curve $d^a$, $d \in [0,1]$, for the conventional gEUD-based constraints (3) we may provide three distinct interpretations for the $a$ parameter given its value, emphasizing the anticipated effect of a particular constraint on the feasible dose distribution:

- if $a \leq 0$, the emphasis is placed on the low-dose part of the distribution; in particular, constraint (3) puts more relative importance on ensuring that there are not too many voxels with small dose values $d_v$; and therefore, this type of constraint is expected to be primarily used for the target volumes;
- if $a \in [0,1]$, the emphasis is also placed on the low-dose part of the distribution; however, unlike the case $a \leq 0$ now constraint (3) puts more relative importance on ensuring that there are not too few voxels with

small dose values $d_v$; and therefore, this type of constraint is expected to be used for the organs at risk;

- if $a \in [1, \infty)$, the emphasis is placed on the high-dose part of the distribution; constraint (3) puts more relative importance on ensuring that there are not too many voxels with high dose values $d_v$; and therefore, this type of constraint is expected to be used for the organs at risk as well.

It is worth mentioning that despite somewhat counter-intuitive interpretation for $a \in [0, 1]$, namely, the reversed sign of the inequality in (3), the constraints of this type prove useful in approximating the desired dose distribution.

In general, the distribution of finite $a$'s selected can be guided by clinical knowledge regarding the serial or parallel nature of the organ at risk or the target.

### 2.2 How to judge the quality of approximating the DVH?

To quantify the quality of the approximation we address the following question: given a set of (convex) GMCs, a desired dose distribution prescribed by the DVH and an energy level $T$, what is the minimal and maximal volume-percentage $P_{\min}(T), P_{\max}(T)$ that may receive dose greater or equal than $T$, subject to these constraints.

To illustrate this concept we refer the reader to the example in the previous subsection: consider $T = \frac{1}{3}$, clearly $\{d_1 = 1/2, d_2 = 1/2\}$ is a feasible distribution and therefore $P_{\max}(T) = 1$, on the other hand, there is no feasible distribution with $d_1, d_2 \leq \frac{1}{3}$ and $d_1 + d_2 = 1$ so $P_{\min}(T) > 0$ while $\{d_1 = 0, d_2 = 1\}$ is feasible and therefore $P_{\min}(T) = \frac{1}{2}$, see Figure 1.

By varying $T$ through the whole range of possible doses for the volume from 0 to the maximum possible dose $D_{\max} = 1$ one may reconstruct the absolute error margins for this type of approximation as

$$\mathrm{DVH}_{\min}(T) = P_{\min}(T),\ \mathrm{DVH}_{\max}(T) = P_{\max}(T),\ T \in [0, 1],$$

meaning that there is no dose distribution that would simultaneously satisfy the set of the given gEUD-type constraints and fall out of the *feasible envelope* spanned by the two curves $\mathrm{DVH}_{\min}, \mathrm{DVH}_{\max}$ containing the original DVH.

Coming back to the illustration, the absolute error margins are formed by connecting with straight segments the points $\{(0, 1/2), (1/2, 1/2), (1/2, 0), (1, 0)\}$ for $\mathrm{DVH}_{\min}$ and $\{(0, 1), (1/2, 1), (1/2, /12), (1, 1/2), (1, 0)\}$ for $\mathrm{DVH}_{\max}$, and contain precisely the feasible envelope (comprising of the two shaded blocks in Figure 1) spanned by two "extreme" distributions corresponding to $\{d_1 = 1/2, d_2 = 1/2\}$ and $\{d_1 = 0, d_2 = 1\}$.

## 3 A probabilistic approach to DVH

In this section we introduce a probabilistic point of view on the dose distribution for the volume of interest, discretized into a collection of $|V|$ voxels, and relate

this perspective to the GMCs – a generalization of conventional gEUD-based constraints.

The fundamental object in the theory of probability is a random variable: an unknown function mapping the space of (random) events into the space of outcomes – the values of this function. The theory studies the properties of the unknown function, the random variable, given some partial information about it. So, from the mathematical point of view there is nothing random about random variables, it is the lack of complete information that we aim to overcome. This is exactly the scenario we are faced with while attempting to understand the properties of the dose distribution, namely the associated DVH, given that the specific values of dose to the voxels, thought of as a random variable -an unknown function assigning the dose value based on the voxel index as an input- are not available, and only some aggregate gEUD-like values are specified.

Let $D$ be a discrete random variable (see, for example, [15]) taking on $|V|$, possibly distinct, values $d_v, v \in V$ all with equal probability of $\frac{1}{|V|}$; think of a $|V|$-faceted die with each face marked with value $d_v, v \in V$. A *cumulative distribution function* (c.d.f.) associated with $D$ at a point $T$ is defined as $F_D(T) = \Pr\{D \leq T\}$ – the probability that the random variable $D$ does not exceed value $T$. Now, observe that the previously defined Dose-Volume Histogram curve satisfies the following important relationship:

$$\mathrm{DVH}(T) = 1 - F_D(T).$$

On the other hand, the gEUD value corresponding to $a$,

$$\mathrm{gEUD}_a = \frac{1}{|V|}{d_1}^a + \frac{1}{|V|}{d_2}^a + \cdots + \frac{1}{|V|}{d_{|V|}}^a,$$

is easily recognized as the *a-moment* of the $D$ random variable. So, indeed, the question of how restrictive are the gEUD-type constraints with regards to the resulting DVH, may be equivalently translated into the question of extracting all possible cumulative distribution functions $F_D$ of discrete random variables $D$ that have their $a$-moments in the given range.

More generally, given a univariate function $f$ and a random variable $D$, one may define an *f-generalized moment* as

$$E[f(D)] = \frac{1}{|V|}f(d_1) + \frac{1}{|V|}f(d_2) + \cdots + \frac{1}{|V|}f(d_{|V|}),$$

and subsequently use the constraints of the form

$$\frac{1}{|V|}\sum_{v \in V} f(d_v) \leq GM_f, \tag{4}$$

hence the term *Generalized Moment Constraint*, to further refine the resulting set of feasible distributions and the corresponding DVH curves. An example of already familiar constraint of this type is $f(d) = d^a$, $a \geq 1$, resulting in a conventional gEUD-based constraint as described before. Finally, note that if $f$

is convex on $[0,1]$, then the resulting constraint (4) is convex as well. In Section 4 we will illustrate that the use of the GMCs allows us to attain the desired set of acceptable DVH's for a particular organ at risk under consideration.

The motivation for generalized gEUD-based constraints is as follows. If we want to control the dose distribution around a critical dose threshold $T$, say on a subset $[\alpha,\beta] \supseteq T$ of $[0,1]$, with help of the moments only, ideally we would use

$$f(d) = \begin{cases} 1, & \text{if } \alpha \le d \le \beta, \\ 0, & \text{otherwise,} \end{cases}$$

for the $f$-generalized moment constraint, since $E[f(D)]$ will have non-zero contributions only from the voxels with dose values in $[\alpha,\beta]$. Consequently, if we wish to bound the number of such voxels from above by $GM_f \cdot |V|$, then inequality (4) would do the job. Likewise, the same inequality with $f$ and $GM_f$ replaced by $-f$ and $-GM_f$ would bound the number of such voxels from below. However, $f$ is not convex, so the convexity of the resulting model would be jeopardized as well.

Instead of the non-convex indicator function $f$ discussed so far, we propose to use an indicator function of $[\alpha,\beta] \subseteq [0,1]$, fused with two monomial functions on $[0,\alpha]$ and $[\beta,1]$, defined with parameters $\ell, r \in [-1,0]$ or $\ell, r \ge 1$:

$$f_{(\alpha,\beta,\ell,r)}(d) = \begin{cases} \left.\begin{array}{ll} -1 & \text{, if } d \in [\alpha,\beta], \\ -\left(\frac{d}{\alpha}\right)^{-\ell} & \text{, if } d \in [0,\alpha], \\ -\left(\frac{1-d}{1-\beta}\right)^{-r} & \text{, if } d \in [\beta,1], \end{array}\right\} & \text{if } \ell, r \in [-1,0], \\ \left.\begin{array}{ll} 0 & \text{, if } d \in [\alpha,\beta], \\ \left(\frac{\alpha-d}{\alpha}\right)^{\ell} & \text{, if } d \in [0,\alpha], \\ \left(\frac{d-\beta}{1-\beta}\right)^{r} & \text{, if } d \in [\beta,1], \end{array}\right\} & \text{if } \ell, r \in [1,\infty), \end{cases}$$

see Figure 2. Clearly, $f_{(\alpha,\beta,\ell,r)}$ is convex, and thus, constraint (4) is convex as well. Function $f_{(\alpha,\beta,\ell,r)}$ may be viewed as a *convex approximation* of the $[\alpha,\beta]$-indicator function $f$, and thus is expected to have a similar effect with regards to controlling the dose distribution, and the $f_{(\alpha,\beta,\ell,r)}$-moments generalize the gEUD values, mean-tail-dose values [7], etc. From the modeling perspective, the choice of $f_{(\alpha,\beta,\ell,r)}$ allows for its efficient embedding into the so-called second-order conic programming problem [2], which is particularly well-suited for efficient computational optimization methods [1]. Moreover, our numerical investigation indicates that these functions nearly exhaust all the convex GMCs that have non-negligible effect on the proximity of feasible dose distributions to the desired DVH.

Perhaps one of the most celebrated relationship between the moments of a random variable and its cumulative distribution function is Tchebychev's inequality, that gives an explicit formula for the probability of a random variable $D$ to deviate in a given range $k\sigma$ from its mean $\mu(= \text{gEUD}_1)$ given the variance

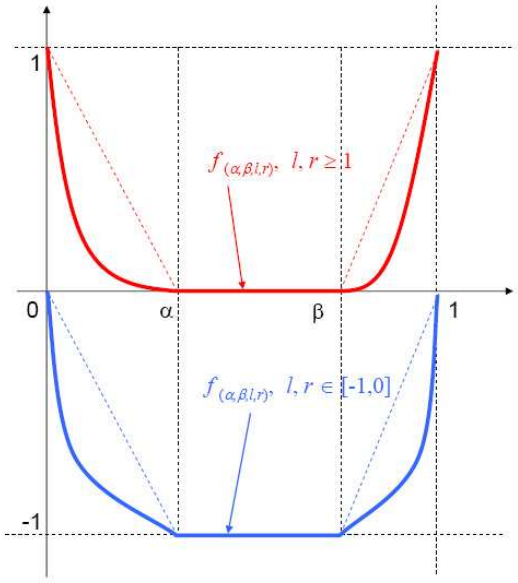


Figure 2: $f_{(\alpha,\beta,\ell,r)}$ for $\ell, r \in [-1, 0]$ and $\ell, r \geq 1$.

$\sigma^2 (= \text{gEUD}_2 - \text{gEUD}_1^2)$, i.e., the first and shifted second moments:

$$\Pr\{|D - \mu| > k\sigma\} < \frac{1}{k^2}.$$

Unfortunately, for higher-order moments such an explicit expression is not available. One has to resort to the use of numerical optimization methods in order to compute the maximum probability mass on a given subset $S \subseteq [0, 1]$, $\Pr_S^{\max}$, over all probability measures $F$ on $[0, 1]$, subject to a set of GMCs:

$$\begin{aligned} & \Pr_S^{\max} := \max \textstyle\int_S dF(x) \\ \text{subject to} \quad & \\ & \textstyle\int_{[0,1]} f_i(x) dF(x) \leq GM_{f_i},\ i = 1, \ldots, m. \end{aligned} \tag{5}$$

The details on how to compute $\Pr_S^{\max}$ are discussed in [17]: we generalize the so-called semi-definite optimization approach of [4] to accommodate our problem formulation, moreover, we provide a natural linear programming relaxation of this problem that proves to be numerically superior in our setting.

The relationship between $\Pr_S^{\max}$ and the error margins provided by $P_{\min}(T)$ and $P_{\max}(T)$ is easily established observing

$$\begin{aligned} & P_{\min}(T) = 1 - \Pr_{[0,T]}^{\max}, \\ & P_{\max}(T) = 1 - (1 - \Pr_{[T,1]}^{\max}) = \Pr_{[T,1]}^{\max} \end{aligned} \tag{6}$$

where the second equality uses the fact that $\Pr\{D \leq T\} = 1 - \Pr\{D > T\}$.

Finally, we mention an important property of the probability distributions that attain $\Pr_S^{\max}$:

**Fact 3.1.** *The maximal probability mass $Pr_S^{\max}$ may always be attained by a piece-wise linear c.d.f., i.e., by a monotone non-decreasing step function with at most $m + 1$ jumps.*

The last property indicates that if we restrict ourselves only to smooth dose distributions for the volume of interest, then the extreme values $\Pr_S^{\max}$ as computed in (5) might not be achievable under this assumption. One may think of adding more constraints to the optimization problem (5) and thus reducing the search space of all feasible c.d.f.'s. Note that, from the practical point of view, the smoothness of the dose distribution is a realistic assumption due to photon and electron scatter, and the use of multiple beam orientations. So, in fact, the true absolute error margins might be tighter than what is predicted by (6).

# 4 A case study

## 4.1 The setup

Consider the following dose-volume criteria for the rectum during treatment of prostate cancer, given by the collection of critical DVH points $(T, P)$ in Table 1. The critical points are further connected with the straight linear segments to

| Dose ($T$), Gy | Volume ($P$), % |
|---|---|
| 20 | 100 |
| 25 | 50 |
| 50 | 30 |
| 60 | 25 |
| 73.8 | 15 |
| 79.2 | 0 |

Table 1: Target for the rectum DVH.

create a corresponding target DVH. Note that at Princess Margaret Hospital the volumes of rectum (and bladder) that are evaluated are limited to 1.8cm superior or inferior of the CTV, thus 20Gy received by the whole rectum volume is considered acceptable.

The design of the target dose prescription and its DVH is a separate subject and goes beyond the scope of this paper, however, we should mention its key guiding principle – the target DVH should be aimed at balancing out the clinical acceptability of the dose distribution with the collection of DVH critical points not being too restrictive at the same time; think of the "worst", but still clinically acceptable dose distribution.

The target DVH is scaled so that the maximum allowed dose is equal to 1 unit, i.e., we scale $T$ by 1/79.2. The set of 13 GMCs is listed in Table 2, each defined as four parameters of $f_{(\alpha,\beta,\ell,r)}$ with the right-hand side $GM_{f_{(\alpha,\beta,\ell,r)}}$ of constraint (4) computed as $E[f_{(\alpha,\beta,\ell,r)}(D)]$, with $D$ corresponding to the target DVH. To interpret those, note that, for example, constraints four through eight

| $\alpha$ | $\beta$ | $\ell$ | $r$ | $GM_{f_{(\alpha,\beta,\ell,r)}}$ |
|---|---|---|---|---|
| 1 | 1 | -0.125 | -1 | 0.9039 |
| 1 | 1 | -0.25 | -1 | 0.8204 |
| 1 | 1 | -.5 | -1 | 0.6843 |
| 0 | 0.2525 | 1 | 1 | 0.5008 |
| 0 | 0.2525 | 1 | 2 | 0.3228 |
| 0 | 0.2525 | 1 | 4 | 0.2104 |
| 0 | 0.2525 | 1 | 8 | 0.1476 |
| 0 | 0.2525 | 1 | 16 | 0.1005 |
| .05 | .3 | -1 | -1 | 0.7004 |
| 0 | 0.9318 | 1 | 1 | 0.0750 |
| 0 | 0.9318 | 1 | 2 | 0.0500 |
| 0 | 0.8585 | 1 | 1 | 0.1247 |
| 0 | 0.7575 | 1 | 1 | 0.1648 |

Table 2: The set of GMCs.

are conventional gEUD-based constraints, while tenth, twelfth and thirteenth are mean-tail dose constraints [7]. The constraints in 2 were selected experimentally, with the choice of parameters partially driven by the clinical knowledge of the nature of the organ.

## 4.2 DVH margins and extreme distributions analysis

We compute the absolute error margins $\text{DVH}_{\min}$ and $\text{DVH}_{\max}$ for the specified set of GMCs, see Figure 4(a).

Although the absolute error margins might look somewhat alarming, a more thorough analysis of the extreme dose distributions reveals much more favorable situation in terms of achieving the desired proximity to the target DVH. While the error margins signify that there are no feasible distributions lying outside of the feasible dose envelope spanned by $\text{DVH}_{\min}$ and $\text{DVH}_{\max}$, there is no feasible dose distribution that will be threateningly close to $\text{DVH}_{\max}$, which may be associated with unacceptable risk of treatment complications. Due to the nature of the selected GMCs, any significant dose escalation above the target DVH on a sub-interval of $[0, 1]$ has to be compensated by the corresponding drop in the dose outside of this interval, thus resulting in much more conservative dose distributions to the rectum volume, see Figure 4(b,c,d,e,f). We depict a few extreme dose distributions that correspond to a sequence of increasing values of dose threshold $T$, and represent three typical dose profiles observed for such

dose distributions: close proximity to the target DVH in (b,c,f), and two (d) or three (e) dose value clusters.

Moreover, neither the beam geometry nor the proximity of the rectum to the target nor the effect of dose scatter were taken into account, all having the potential to further restrict the set of feasible DVH's, and thus, to improve the quality of approximating the target DVH with the set of GMCs described.

## 4.3 GMC model formulation

We describe how to embed the GMCs into a particularly well structured optimization problem, the second-order conic optimization problem

$$\begin{array}{rl} & \min c^T x \\ \text{subject to} & \\ & Ax = b, \\ & x \in K, \end{array}$$

where $c, x \in \mathbb{R}^n$, $b \in \mathbb{R}^m$, $A$ is $m \times n$ real matrix, and $K$ is an $n$-dimensional second-order cone, also known as Lorentz cones,

$$SOC = \left\{ x \in \mathbb{R}^n : x_n \geq \left( \sum_{j=1}^{n-1} x_j^2 \right)^{1/2} \right\},$$

or, more generally, $K$ is a direct product of $k$ distinct second-order cones, $K = SOC_1 \times SOC_2 \times \cdots \times SOC_k$, so that their dimensions add up to $n$. Note that the second-order conic optimization problem allows to specify nonnegative variables by using 1-dimensional second-order cones.

The optimization problem as above is amenable to very efficient computational optimization methods, the so-called interior-point methods [1, 2, 14]. To name a few most successful numerical optimization packages that are capable of solving such problems, we mention a commercial solver Mosek (mosek.com), and freeware packages SDPT3 (www.math.nus.edu.sg/∼mattohkc/sdpt3.html) and SeDuMi (sedumi.mcmaster.ca).

Constraint (4) with convex $f = f_{(\alpha,\beta,\ell,r)}$ may be re-written as

$$\begin{array}{c} f_{(\alpha,\beta,\ell,r)}(d_i) \leq \Psi_i,\ i = 1, \ldots, |V|, \\ \displaystyle\sum_{i=1}^{|V|} \Psi_i \leq |V| \cdot GM_f. \end{array} \tag{7}$$

In particular, we focus on the case $|\ell|, |r|$ being integer powers of 2, e.g., $\ell = -1/4, -1/2, -1, 1, 2, 4$, etc. This restriction significantly simplifies the representation of the GMCs as second-order conic constraints, and from the practical point of view of approximating the desired DVH does not seem to have any substantial negative implications. For a representation of the epigraph of $f_{(\alpha,\beta,\ell,r)}$ with arbitrary rational values of $\ell, r \in [-1, 0] \cup [1, \infty)$ see [2].

Note that the second constraint in (7) may be easily handled by introducing a non-negative slack variable $s \geq 0$ by $\sum_{i=1}^{|V|} \Psi_i + s = |V| \cdot GM_f$. It is left to show how to represent $f_{(\alpha,\beta,\ell,r)}(d_i) \leq \Psi_i$ for each $i = 1, \ldots, |V|$.

Let us fix $i$, and consider

$$f_{(\alpha,\beta,\ell,r)}(d_i) \leq \Psi_i. \tag{8}$$

Let $p_\ell, p_r$ be two nonnegative integers so that either $\ell = -2^{-p_\ell}, r = -2^{-p_r}$ or $\ell = 2^{p_\ell}, r = 2^{p_r}$. The procedure below allows to represent constraint (8) -the epigraph of $f_{(\alpha,\beta,\ell,r)}$ for $d_i \in [0,1]$- as a second-order conic constraint. We need $(4p_\ell + 2)$ additional variables, $2p_\ell + 2$ second-order cones and $3p_\ell + 1$ linear constraints for the $\ell$-monomial branch of $f_{(\alpha,\beta,\ell,r)}$ on $[0,\beta]$. Similarly, we need $(4p_r + 2)$ additional variables, $2p_r + 2$ second-order cones and $3p_r + 1$ linear constraints for the $r$-monomial branch of $f_{(\alpha,\beta,\ell,r)}$ on $[\alpha,1]$. In addition, we use 2 more non-negative slack variables, and thus 2 more second-order cones, with 2 additional linear constraints, to merge the two branches together to obtain (8).

Case 1: $\ell, r \in [1,\infty)$, that is, $\ell = 2^{p_\ell}, r = 2^{p_r}$.

We start with constructing partial constraint to (8) that corresponds to

$$f_{(\alpha,\beta,\ell,r)}(d_i) \leq z_{p_\ell},\ d_i \in [0,\beta] \subseteq [0,1]. \tag{9}$$

Introduce $z_0 \geq \max\left\{0, \frac{\alpha - d_i}{\alpha}\right\}$ by

$$\begin{array}{l} \frac{1}{\alpha} d_i + z_0 + s_0 = 1, \\ z_0, s_0 \geq 0. \end{array} \tag{10}$$

Note that this requires 2 additional nonnegative variables, and thus, 2 additional 1-dimensional second-order cones $SOC_1, SOC_2$, and 1 linear constraint.

Observe that if $(\xi_1,\xi_2,\xi_3) \in SOC = \left\{(\xi_1,\xi_2,\xi_3) \in \mathbb{R}^3 : \xi_3 \geq \sqrt{\xi_1^2 + \xi_2^2}\right\}$, then by considering the planar slice of the second-order cone $SOC$ along $\xi_3 - \xi_2 = 1$, noting that $\xi_1^2 + \xi_2^2 \leq \xi_3^2 \Leftrightarrow \xi_1^2 \leq (\xi_3 + \xi_2)(\xi_3 - \xi_2)$, we have $\xi_1^2 \leq \xi_2 + \xi_3$, an epigraph of a branch of parabola in variables $\xi_1 \in \mathbb{R}$ and $(\xi_2 + \xi_3) \geq 0$, see Figure 3.

Now, for $k = 1, \ldots, p_\ell$ let

$$\begin{array}{rll} -z_k & +\xi_{2,k} + \xi_{3,k} & = 0, \\ & -\xi_{2,k} + \xi_{3,k} & = 1, \\ z_{k-1} & -\xi_{1,k} & = 0, \\ z_k \geq 0,\ (\xi_{1,k},\xi_{2,k},\xi_{3,k}) & \in SOC_{k+2} \subset \mathbb{R}^3, & \end{array} \tag{11}$$

this requires $4p_\ell$ additional variables, $p_\ell$ 3-dimensional and $p_\ell$ 1-dimensional second-order cones, and $3p_\ell$ linear constraints. Observe that combining (10) with (11) we have exactly $f_{(\alpha,\beta,\ell,r)}(d_i) \leq z_{p_\ell}$ for $d_i \in [0,\beta]$.

Similarly, we may construct a partial constraint to (8) that corresponds to

$$f_{(\alpha,\beta,\ell,r)}(d_i) \leq z_{p_r},\ d_i \in [\alpha,1] \subseteq [0,1], \tag{12}$$

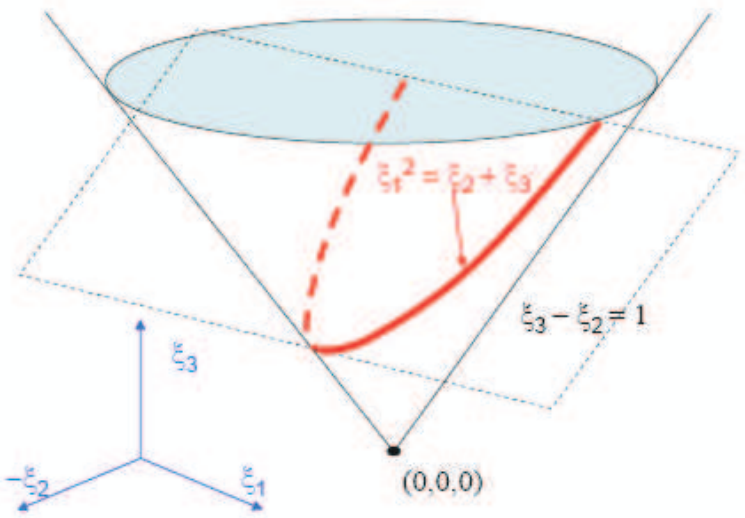


Figure 3: A branch of parabola as a section of $SOC$ cone.

by replacing $z_0 \geq \max\left\{0, \frac{\alpha - d_i}{\alpha}\right\}$ with $z_0 \geq \max\left\{0, \frac{d_i - \beta}{1-\beta}\right\}$ in a new independent instance of (10), and adding a new independent set of constraints (11) with $k = 1, \ldots, p_r$.

Finally, to merge the branches (9) and (12) together, we write $\Psi_i \geq z_{p_\ell}$, $\Psi_i \geq z_{p_r}$ by introducing two more non-negative slack variables with two linear constraints

$$\begin{aligned} \Psi_i - z_{p_\ell} + \nu_1 &= 0, \\ \Psi_i - z_{p_r} + \nu_2 &= 0, \\ \nu_1, \nu_2 &\geq 0. \end{aligned} \tag{13}$$

Case 2: $\ell, r \in [-1, 0]$, that is, $\ell = -2^{-p_\ell}, r = -2^{-p_r}$.

Constraint (8) may be represented in almost the same way as in the previous case, with the following exceptions.

- In (10), we replace $z_0 \geq \max\left\{0, \frac{\alpha - d_i}{\alpha}\right\}$ and $z_0 \geq \max\left\{0, \frac{d_i - \beta}{1-\beta}\right\}$ with $z_0 \leq \min\left\{1, \frac{d_i}{\alpha}\right\}$, i.e., $\frac{-1}{\alpha} d_i + z_0 - s_0 = 0$, $z_0 \leq 1$, $s_0 \geq 0$, and $z_0 \leq \min\left\{1, \frac{1-d_i}{1-\beta}\right\}$ for the $\ell$ and $r$-monomial branches of $f_{(\alpha,\beta,\ell,r)}$, respectively. Note that the constraint $z_0 \leq 1$ may be easily recast as a nonnegativity constraint $\zeta_0 \geq 0$ by replacing $z_0$ with $-\zeta_0 + 1$.

- In (11), we interchange the roles of $z_k$ and $z_{k-1}$ and replace the nonnegativity constraint on $z_k$ by $z_k \leq 1$, that is, depending on the monomial

branch, for $k = 1, \ldots, p_\ell$ or $k = 1, \ldots, p_r$, we let

$$\begin{array}{lll} -z_{k-1} & +\xi_{2,k} + \xi_{3,k} & = 0, \\ & -\xi_{2,k} + \xi_{3,k} & = 1, \\ z_k & -\xi_{1,k} & = 0, \\ z_k \leq 1, \ (\xi_{1,k}, \xi_{2,k}, \xi_{3,k}) \in SOC_{k+2} \subset \mathbb{R}^3. & & \end{array}$$

Again, the constraint $z_k \leq 1$ may be easily recast into nonnegativity of $\zeta_k$ by letting $z_k = -\zeta_k + 1$;

- Finally, we replace (13) by

$$\begin{array}{c} \Psi_i + z_{p_\ell} - \nu_1 = 0, \\ \Psi_i + z_{p_r} - \nu_2 = 0, \\ \nu_1, \nu_2 \geq 0. \end{array}$$

Note that $z_{p_\ell}$ and $z_{p_r}$ bounds $-f_{(\alpha,\beta,\ell,r)}$ from below on $[0, \beta]$ and $[\alpha, 1]$, so we need to change the sign of $\Psi_i$ as compared to (13).

# 5 Conclusion and future work

We investigate the use of the multiple GMCs, as the means to control the proximity of the planned dose distribution to the desired idealized dose prescription. The newly proposed approach is promising as demonstrated by the computational study where the rectum DVH is considered. Unlike the precise dose-volume constraint formulation that uses mixed integer programming techniques and in practice often necessitates the use of expensive super-computing resources, e.g., [10], our convex optimization approach is more likely to be suitable for clinical implementation, since the resulting optimization model is amenable to highly-efficient optimization methods that may be implemented on even a single-processor computing station.

The future work in this direction includes the following goals:

- computational comparison of GMC-based IMRT optimization approach with conventional treatment planning formulations,
- investigation of practically relevant OAR and target partial dose-volume constraints to identify a subclass of dose distributions suitable to GMC-based approximation,
- embedding of GMC approximation toolbox for DVH in CERR [8], enhanced with the database of current DVH/GMC conversion protocols for selected target and OAR DVH's.

# Appendix

We discuss the interplay between the gEUD values and the DVH, as stated in Fact 1.1, in a bit more details. Namely, we introduce one as the Taylor

expansion coefficients of the Fourier transform of the other. Thus, roughly speaking, the restriction of the feasible dose distributions to only the ones that satisfy a particular finite set of GMCs may be viewed as equivalent to considering only the specified Fourier coefficients in the expansion of the corresponding DVH's. We state a more general classical result from probability theory and draw the conclusion of Fact 1.1 as its corollary.

For simplicity, here we assume the dose distribution, represented by a random variable $D$, to have a corresponding DVH with no jumps, i.e., a continuous function, moreover, we assume the derivative of the DVH curve also changes continuously – think of describing the dose to a volume of interest in the limiting case when the volume of each voxel goes to 0. With this assumption, $D$ is a continuous random variable. The discussion below may be extended to a more general case of DVH's with jumps, for the corresponding rigorous probabilistic argument see the chapter on characteristic functions in [15].

Recall that $D$ is a continuous random variable if we can write

$$\Pr\{D \leq T\} = F_D(T) = \int_{-\infty}^{T} f_D(\xi) d\xi$$

for some $f_D(\xi) \geq 0$, $f_D(\xi)$ is called a probability density function of $D$. We say that $D$ is supported on $[0, M]$ if $f_D(\xi)$ may be taken to be 0 outside of $[0, M]$, in the later case we can also write

$$F_D(T) = \int_{0}^{T} f_D(\xi) d\xi.$$

Given $D$, its moment-generating function is defined as

$$M_D(t) = \int_{-\infty}^{\infty} e^{t\xi} dF_D(\xi) = \int_{-\infty}^{\infty} e^{t\xi} f_D(\xi) d\xi$$

if there exists $h > 0$ such that $M_D(t) < \infty$ for $|t| < h$. Note that if $D$ is supported on a finite interval $[0, M]$, i.e., has a compact support, $M_D(t)$ is well-defined for all $t$.

An important property of the moment-generating function of $D$ is that its $k$-th derivative at 0 satisfies

$$M_D^{(k)}(0) = \int_{-\infty}^{\infty} \xi^k f_D(\xi) d\xi = E[D^k],$$

where $E[D^k]$ is referred to as the $k$-th moment of $D$. Observe that the last identity may be verified by switching the order of differentiation and integration and using dominated convergence theorem. If $D$ has a compact support, $M_D(t)$ is real-analytic and thus may be expanded into converging Taylor series around 0 for any $t$:

$$M_D(t) = 1 + E[D] \cdot t + \frac{E[D^2]}{2!} \cdot t^2 + \frac{E[D^3]}{3!} \cdot t^3 + \cdots .$$

Note that the sequence $\{E[D^k]\}_{k=0,1,2,\ldots}$ defines $M_D(t)$ uniquely.

The Fourier transform [16] of $f_D(\xi)$ is defined as

$$\mathcal{F}[f_D(\xi)](\omega) = \widehat{f}_D(\omega) = \frac{1}{\sqrt{2\pi}} \int_{-\infty}^{\infty} e^{-i\omega\xi} f_D(\xi) d\xi,$$

with its inverse transform

$$\mathcal{F}^{-1}[\widehat{f}_D(\omega)](\xi) = \frac{1}{\sqrt{2\pi}} \int_{-\infty}^{\infty} e^{i\omega\xi} \widehat{f}_D(\omega) d\omega.$$

Recall that a sufficient condition for

$$\mathcal{F}^{-1}[\mathcal{F}[f_D(\xi)](\omega)](\xi) = f_D(\xi)$$

with continuous $f_D(\xi)$ is absolute integrability of $f_D(\xi)$, that is

$$\int_{-\infty}^{\infty} |f_D(\xi)| d\xi < \infty.$$

A more general analogue of $\widehat{f}_D(\omega)$ as above called *$F_D$-characteristic function* may be found in [15].

**Theorem 5.1 (Theorem 9.5.1 and its corollary, [15]).** *If $F_D$ is a probability distribution with an absolutely-integrable characteristic function $\Phi$, then $F_D$ has a bounded continuous density $f_D = \frac{1}{\sqrt{2\pi}} \widehat{\Phi}$.*

Now, observe that if $D$ is a continuous random variable with compact support in $[0, M]$ and a continuous density $f_D(\xi)$, then we may recover the probability distribution of $D$ from its moment generating function which is uniquely determined by $E[D^k]$ moments of $D$. To understand this, note that

$$M_D(t) = \sqrt{2\pi} \mathcal{F}[f_D(\xi)](it),$$

and since the absolute integrability is clearly satisfied for $f_D(\xi)$, defined as

$$f_D(\xi) = \frac{1}{2\pi} \int_{-\infty}^{\infty} e^{i\omega\xi} M_D(-i\omega) d\omega.$$

Therefore, as a consequence of the theorem above we have

**Corollary 5.1.** *If $D$ is a continuous random variable on $[0, 1]$ with a continuous density function $f_D(\xi)$, then there is one-to-one correspondence between the sequence of moments of $D$, $\{E[D^a]\}_{a=1,2,\ldots}$, and its c.d.f. $F_D$.*

Finally, to establish the Fact 1.1, we have to refine our definition of gEUD values. Let

$$\widetilde{\text{gEUD}}_a = \int_0^1 \xi^a dF(\xi),$$

and note that a more customary definition of gEUD values, presented at the beginning of this paper, corresponds to a discrete approximation of the integral above, based on voxel-based dose distribution approximation. To get arbitrarily close approximation to the $\widetilde{\text{gEUD}}_a$, one may think of setting voxel volume asymptotically close to 0.

Now, observe that indeed, due to physical properties and limitations of the dose distribution, the following holds true.

- The ratio of the dose to a voxel by the voxel volume is confined to a bounded interval, i.e., it is non-negative and is bounded from above by some absolute maximum. If nothing else, imposed by the technical capabilities of a linac.
- In the limiting case of voxel volume going to 0, due to scatter the DVH histogram is a sufficiently smooth curve.

Therefore, the corollary above is applicable and we have one-to-one correspondence between $\left\{\widetilde{\text{gEUD}}_a\right\}_{a=1,2,\ldots}$ and $\text{DVH}(T) = 1 - F_D(T)$, $T \in [0,1]$.

Strictly speaking, Fact 1.1 should have been stated in terms of $\widetilde{\text{gEUD}}_a$ values. However, since $\text{gEUD}_a$ approximates $\widetilde{\text{gEUD}}_a$ arbitrarily close for small enough voxel resolution, and Fact 1.1 is used only for motivation, the later gEUD value definition refinement was purposefully omitted to ease the presentation of our approach.

# References


[1] Andersen E., Roos C., Terlaky T.: On implementing a primal-dual interior-point method for conic quadratic optimization, Math. Prog. 95-2 (2003) 249–277

[2] Ben-Tal A., Nemirovski A.: Lectures on modern convex optimization: analysis, algorithms, engineering applications, SIAM, 2001

[3] Beong C., Deasy J.: The generalized equivalent uniform dose function as a basis for intensity-modulated treatment planning, Phys. Med. Biol. 47 (2002) 3579–3589

[4] Bertsimas D., Popescu I.: Optimal inequalities in probability theory: a convex optimization approach, SIAM J. Opt. 15-3 (2005) 780–804

[5] Chan T., Bortfeld, T., and Tsitsiklis J.: A robust approach to IMRT optimization, Phys. Med. Biol. 51 (2006) 2567–2583

[6] Chu M., Zinchenko Y., Henderson S. and Sharpe M.: Robust optimization for intensity modulated radiation therapy treatment planning under uncertainty, Phys. Med. Biol. 50 (2005) 5463–5477

[7] Clark V., Chen Y., Wilkens J., Alaly J., Zakaryan K., and Deasy J.: IMRT treatment planning for prostate cancer using prioritized prescription optimization and mean-tail-dose functions, Lin. Alg. Appl., to appear (2007)

[8] Deasy J., Blanco A., Clark V.: CERR: A computational environment for radiotherapy research, Med. Phys. 30 (2003) 979–985

[9] Lee E., Deasy J.: Optimization in intensity-modulated radiation therapy, SIAG/OPT Opt. in Medicine 17-2 (2006) 20–32

[10] Lee E., Fox T., Crocker I.: Simultaneous beam geometry and intensity map optimization in intensity modulated radiation therapy, Int. J. Radiat. Oncol. Biol. Phys. 64-1 (2006) 301–320

[11] Niemierko A.: Reporting and analyzing dose distributions: A concept of equivalent uniform dose, Med. Phys. 24 (1997) 103-110

[12] Olafsson A., Wright S.: Efficient schemes for robust IMRT treatment planning, Phys. Med. Biol. 51 (2006) 5621-5642

[13] Qiuwen W., Mohan R., Niemierko A.: IMRT optimization based on the generalized equivalent uniform dose(EUD), Proceedings of 22nd Annual International Conference of the IEEE 1 (2000) 710–713

[14] Renegar, J.: A mathematical view of interior-point methods in convex optimization, SIAM, 2001

[15] Resnick S.: A probability path, Birkhauser, 1998

[16] Rudin W.: Real and complex analysis, McGraw-Hill, 1987

[17] Zinchenko Y.: Generalized Tchebychev's inequalities for Hausdorff random variables: a practical convex optimization approach, in preparation (2007)

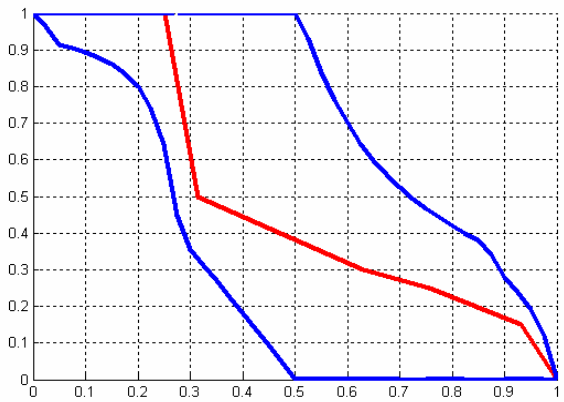

(a) the absolute error bounds (blue curves), spanning the envelope containing the target DVH (red curve)

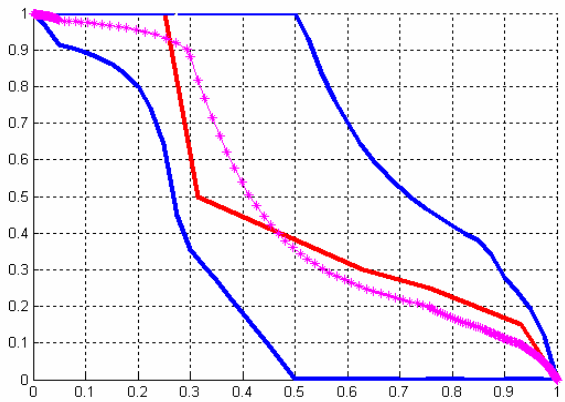

(b) the extreme feasible DVH (in purple) represents a good rectal DVH that is clinically achievable and meets all relevant dose-volume criteria

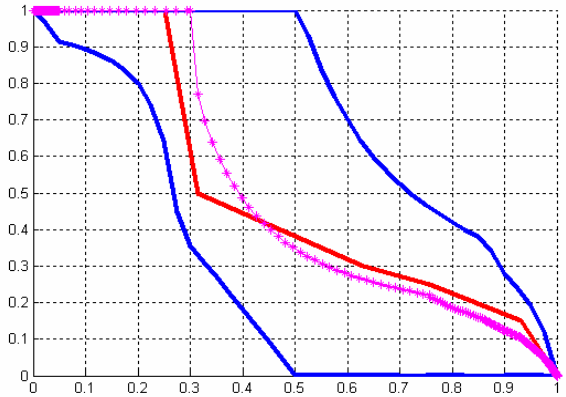

(c) the extreme feasible DVH (in purple) represents a good rectal DVH that is clinically achievable and meets all relevant dose-volume criteria. The large volume receiving a low dose is not likely to be of clinical significance.

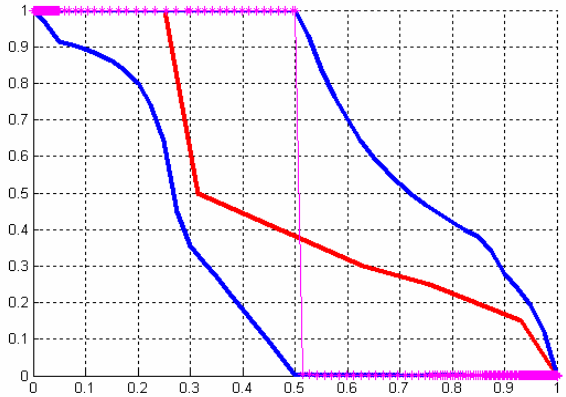

(d) the extreme feasible DVH (in purple) represents a good rectal DVH that is clinically achievable and meets all relevant dose-volume criteria. The proximity of the rectum to the prostate suggest the high dose portion of this DVH may not be entirely achievable.

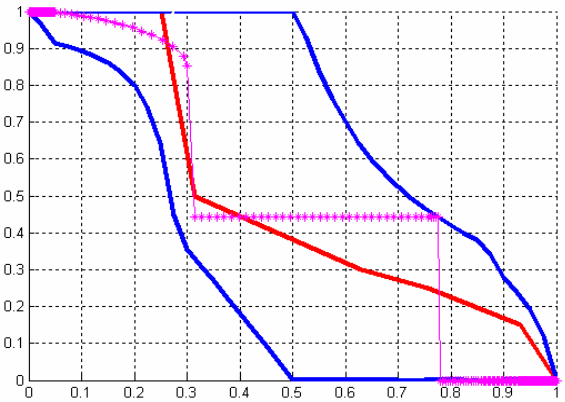

(e) the extreme feasible DVH (in purple) represents a good rectal DVH. The dose received by 45% of the volume exceeds the normal dose-volume criteria, however, this is balanced with exceptional sparing of the high dose volume. The proximity of the rectum to the prostate suggest the high dose portion of this DVH may not be entirely achievable.

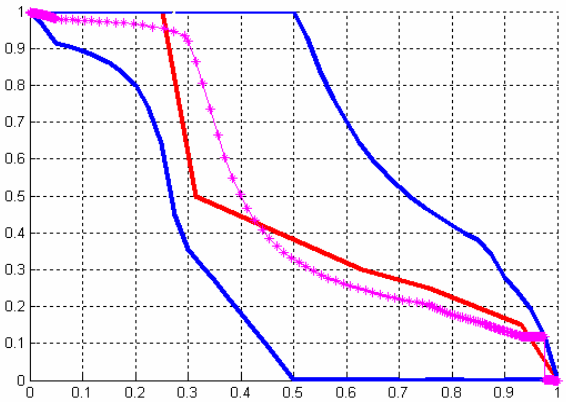

(f) the extreme feasible DVH (in purple) represents a good rectal DVH that is clinically achievable and meets all relevant dose-volume criteria. The proximity of the rectum to the prostate suggest the intermediate dose portion of this DVH may not be entirely achievable.

Figure 4: DVH margins and extreme distributions for the set of GMCs.